Catalysis Today 155 (2010) 147–153

Contents lists available at ScienceDirect

Catalysis Today

journal homepage: www.elsevier.com/locate/cattod

Catalytic combustion of VOC in a counter-diffusive reactor

N. Jodeiri, L. Wu, J. Mmbaga, R.E. Hayes *, S.E. Wanke

Department of Chemical and Materials Engineering, University of Alberta, 116 Street, Edmonton, Alberta, Canada T6G 2G6

ARTICLE INFO

Article history:
Available online 7 January 2009

Keywords:
Catalytic combustion
Radiant heater
Methane

ABSTRACT

This paper presents the results of an experimental investigation on the performance of a counter-diffusive radiant heater used for the combustion of methane and BTEX compounds. The effect of natural gas feed rate on its fractional conversion was studied and it was found that as the feed rate increases the conversion drops, owing to a lack of oxygen for combustion. The effect of oxygen deficiency was confirmed by increasing the air circulation rate in front of the catalyst pad using a fan. The effect of oxygen limitation was also verified by addition of increasing concentrations of pentane to the reactor that led to reduced methane conversion. Suitability of counter-diffusive radiant heater for treatment of natural gas dehydration process effluent was investigated by addition of water, pentane and toluene to the natural gas used as reactor feed. It was found that presence of water does not have a significant negative impact on catalyst activity when added as a vapour, and when other hydrocarbons are present in the feed stream, complete hydrocarbon conversion can be achieved by satisfying the oxygen demand.

1. Introduction

Natural gas contains water vapour that needs to be removed prior to transport to prevent pipeline corrosion and formation of solid hydrates. Typically, water is removed using tri-ethylene glycol in a glycol dehydration unit. During the glycol dehydration process tri-ethylene glycol not only absorbs water, but also methane and other volatile organic compounds, including hazardous air pollutants such as benzene, toluene, ethyl benzene and xylene (collectively known as BTEX). When the glycol is regenerated, these emissions are released. Natural gas dehydration effluent is the third largest methane emission source in the natural gas production industry [1]. Although non-toxic, methane is the second largest contributor to greenhouse gas (GHG) emissions, primarily because it has a global warming potential 23 times that of CO_2, based on a 100-year lifecycle [2–4]. BTEX emissions are generally toxic and their release into the atmosphere is controlled by government regulation. The conventional method of dealing with these emissions is homogeneous combustion in a flare. However, formation of NO_X compounds owing to high operating temperatures cannot be avoided [5–8] and there is a possibility of water and hydrocarbons condensation in the flare, causing smoke formation and incomplete combustion [9]. Catalytic combustion is an alternative to homogeneous combustion and, because it takes place at low temperatures, formation of NO_X does not occur.

A wide variety of catalytic reactors are used for combustion, with the most common being the monolith honeycomb. A significant challenge, especially for low temperature feed, is to achieve auto-thermal operation. In the case where a fuel rich stream is used, the counter-diffusive reactor can be employed. These devices have most commonly been used in radiant heater applications, where the generated energy is removed from the reactor via radiation. The cross-section of a typical unit is shown in Fig. 1. Essentially, the reactor consists of a square catalyst pad contained in a metal housing. Pure fuel is supplied from the back of the pad through a fuel distributer. The fuel flows by convection through the catalyst, and oxygen for combustion is supplied by diffusion from the air. An electrical heater is used to bring the pad to ignition temperature. Usually there is an insulation blanket behind the catalyst pad (fuel injection side) to reduce heat loss through the back of the heater. Most of the energy from the combustion is lost by radiation from the front of the catalytic reactor; hence the name is radiant heater. This design has been widely used in industry for a variety of applications, with both methane and other light hydrocarbons being used as fuel.

Several investigations have been reported in the literature. Sadamori [10] used a rhodium impregnated porous alumina fibre mat to investigate the temperature distribution and gas phase composition as a function of position in the pad for different feed compositions. He found that the maximum temperature within the catalyst layer corresponds to the point where oxygen and methane are consumed. With increasing heat load, the position of maximum temperature moved to the surface, suggesting that the combustion is controlled by oxygen diffusion into the catalyst pad. Application of these devices has also been studied for the heating system of PVC

* Corresponding author.
E-mail address: bob.hayes@ualberta.ca (R.E. Hayes).

0920-5861/$ – see front matter © 2008 Elsevier B.V. All rights reserved.
doi:10.1016/j.cattod.2008.11.015

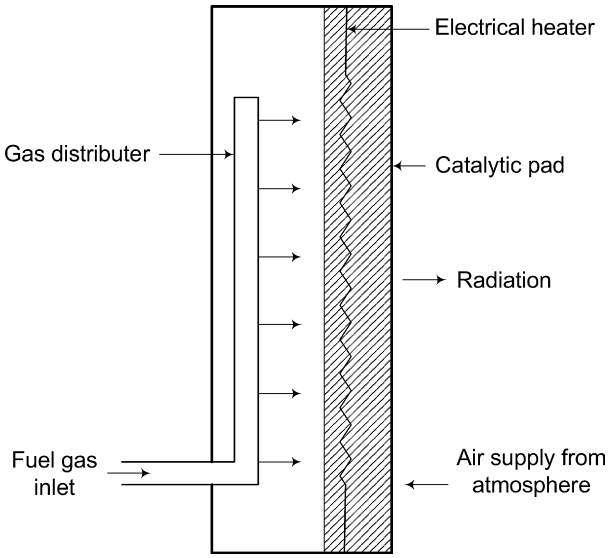

Fig. 1. Cross-section of a typical counter-diffusive radiant heater.

tiles and depending on the installation mode, combustion efficiency as high as 99.5% can be achieved [8].

Seo et al. [7] studied the performance of catalytic burner for drying of acrylic coatings on textiles. During textile coating processes, acrylic resin dissolved in toluene is coated on textiles and the textile is dried using hot air. The toluene mixture evolved during the process is incinerated by flame combustion by supplying additional fuel. They used a catalytic burner with propane as fuel to start up the coating process and when steady state was reached fuel was switched to toluene mixture produced from the drying chamber. The catalyst used was Pt deposited on Al_2O_3 fibres. The counter-diffusive mode was used when the fuel was propane. It was found that vertical and upward installation of the unit led to maximum efficiency and increasing the heat flux reduced the efficiency. In the downward installation, hot combustion gases are stagnant under the pad surface and this limits the oxygen diffusion into the pad. They suggested two ways for improving the efficiency for the downward installation mode: one, supplying the air by forced convection to the front of the catalyst pad, and two, using premixed fuel/oxygen mixtures as feed. It was found that high combustion efficiency can be achieved by using the forced convection but premixed combustion feed led to unacceptable high catalyst temperatures. They concluded that by using the catalytic burner for drying of textile coatings not only is energy saved by recovering the waste heat from toluene, but also emission of pollutants such as NO_X is reduced owing to low operating temperatures.

Radiant heaters have many applications in the oil and gas industry, for example, space heating for well site buildings, compressor sites and oil batteries [11]. One application is combustion of natural gas released at heavy oil wellheads. For wells located in remote areas where shipping of the gas is not economical, the gas can be captured and combusted. The energy generated can be used for heating, which realizes additional benefits in energy savings.

This paper reports the results of an experimental investigation into the use of counter-diffusive reactor for the destruction of the emissions from a natural gas glycol dehydration unit. This effluent stream consists of a mixture of methane, BTEX, water and other hydrocarbons. The effects of fuel flow rate and composition on the destruction efficiency are reported, with particular attention paid to the effects of added water.

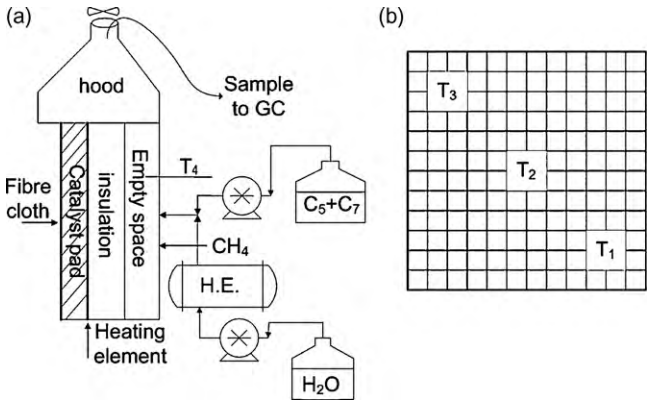

Fig. 2. (a) Cross-sectional view and (b) front view of the counter-diffusive radiant heater; H.E. in (a) and GC in (b) represent heat exchanger and gas chromatograph, respectively.

2. Experimental apparatus and procedures

All of the results reported herein were obtained on a small commercial radiant heater, suitably adapted to allow for variable fuel flow rate and composition. Fig. 2a and b show the cross-section and front view of a counter-diffusive radiant heater. The unit measured 30 cm^2 and was 5.5 cm in depth. It consisted of an empty space for fuel injection, an insulation blanket, an electrical heating element, and an alumina catalyst pad containing platinum as the active ingredient. A woven fibre cloth and metal grid (wire mesh) were used at the front of the system to support the catalyst pad and enhance structural integrity. The thickness of catalyst layer was about 1 cm. A funneling hood was used to collect the exhaust gas, and the sample of exhaust gas was injected to a gas chromatograph (HP 5890) for analysis. The gas chromatograph column was Haysep Q from SUPELCO with helium from Praxair as the carrier gas.

The dehydrator effluent contains a mixture of hydrocarbons and water, with a typical composition given in Table 1. Rather than use this composition, a set of model compounds were substituted. Toluene (C_7) was used to represent the BTEX, while pentane (C_5) was used to represent other non-methane hydrocarbons (NMHC). Municipal natural gas (97.4% methane) was used as the methane supply. Pentane used in the experiments was anhydrous pentane of 99+% purity supplied by Sigma–Aldrich, and toluene was HPLC grade from Fisher Scientific. Natural gas was injected into the reactor using the standard fuel inlet of the heater. The pentane, toluene and water were injected into the back of the heater through a small injection port added to the unit. A digital pump,

Table 1
Composition of glycol regeneration effluent.

Component	Amount (vol.%)
Water	40.4
CH_4	40.1
C_2H_6	6.37
C_3H_8	4.6
i-C_4H_{10}	0.685
n-C_4H_{10}	1.84
i-C_5H_{12}	0.521
n-C_5H_{12}	0.607
Benzene	0.541
Toluene	0.762
Xylenes	0.435
CO_2	0.541
N_2	0.208
Methylcyclohexane	0.399
Ethylbenzene	0.197
Hexanes+	1.794

LabAlliance Series II was used to pump the water, and an ISCO Model 500D syringe pump was used for the pentane and toluene mixture. These two streams joined together shortly before the injection port. To investigate the effect of feed inlet state (liquid or vapour), a shell and tube heat exchanger was used to evaporate the water feed before injection. Hot oil from an oil bath was used on the shell side of the exchanger, while the water passed through the tube side. The temperature of the oil bath was set to 150 °C. A thermocouple was used to monitor the temperature in the feed line to ensure that the water had vapourized.

The temperature of the catalyst pad at depth of 5 mm from the surface was monitored by three thermocouples positioned diagonally in the middle, lower right corner and upper left corner of the unit (see Fig. 2b). Another thermocouple monitored the temperature in the back space where fuel and other compounds are introduced (Fig. 2a).

To study the effect of oxygen mass transfer through the natural convection boundary layer that forms at the pad face, a small 12 V DC fan was installed on top of the funneling hood to increase the convective oxygen flow in front of the catalyst pad. The speed of the fan was adjusted by changing the voltage of the power supply.

To operate the radiant heater, the catalyst pad was preheated using the electrical heating element. When the catalyst pad temperature was high enough to sustain combustion, fuel flow to the system commenced. After the fuel was ignited the electrical heater is turned off.

Labview software package was used for data acquisition. Temperature and methane feed rate data were recorded at user defined time intervals.

3. Results and discussion

3.1. Effect of feed rate on methane conversion and role of oxygen supply

The first result shown is the temperature response of the reactor during base case start-up and operation. The base case operates at a natural gas flow rate of 1.8 g/min. Fig. 3 shows the response of the thermocouples. It is observed that the temperature at the bottom of the catalyst pad is higher compared to the middle and top temperatures. It was initially hypothesized that the temperature distribution observed might result from variations in catalyst activity within the pad, or to the location of the feed pipe. The temperature distribution was subsequently measured at three different pad orientations. In each new test, the heater was rotated 90 degrees, thus the effects of non-uniform catalyst distribution or feed point would be accounted for. It was observed that the temperature distribution was essentially the same for each orientation, and therefore, the temperature distribution effect is attributed to the boundary layer development at the front of the pad, and the subsequent mass transfer limitation of oxygen transport.

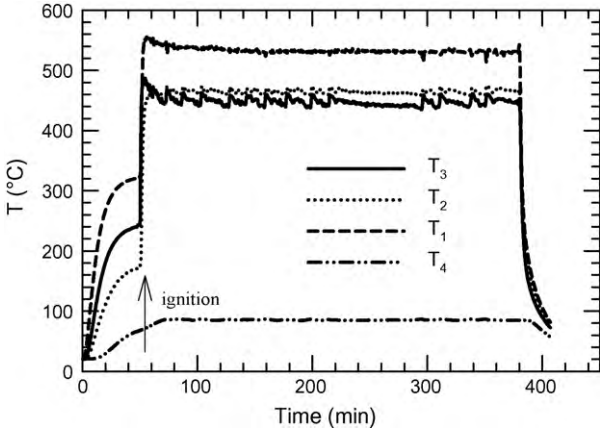

Fig. 3. Temperature profile across the catalyst pad at natural gas feed rate of 1.8 g/min.

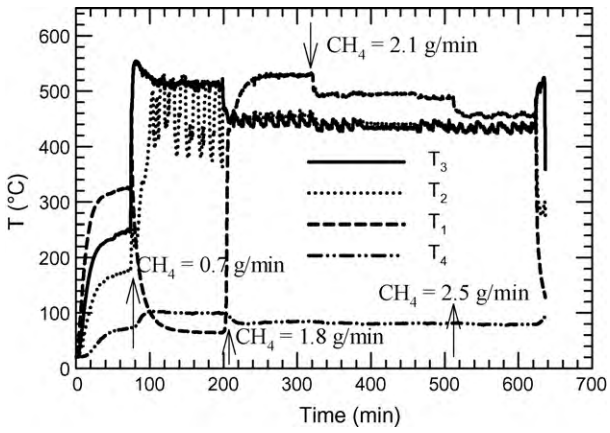

Fig. 4. Temperature profile across the catalyst pad at varying natural gas feed rates.

The next result presented shows the effect of varying the natural gas flow rate. Temperature profile across the catalyst pad at different methane flow rates is shown in Fig. 4. When low flow rate of methane is introduced into the reactor (0.7 g/min), the temperature at the bottom of the pad declined sharply, and combustion was not sustained there. When the flow rate was raised to 1.8 g/min, the lower corner temperature rose rapidly, and the same profile that was observed in Fig. 3 was seen. Increasing the flow rate to 2.1 and then to 2.5 g/min, results in a slight reduction in the temperature at the bottom of the pad.

The conversion of methane in the system was computed from the ratio of methane and carbon dioxide in the effluent, as shown in Eq. (1):

$$\text{CH}_4 \text{ conversion} = \frac{1}{1 + ([\text{CH}_4]/[\text{CO}_2])} \quad (1)$$

where $[CH_4]$ and $[CO_2]$ are the concentrations of methane and carbon dioxide in the reactor exhaust.

Fig. 5 gives the methane conversion as a function of natural gas feed rate. Each data point is the average of several exhaust gas sample analyses at steady state at each feed rate. It was observed that increasing methane feed rates resulted in decreasing methane conversion. Fig. 6 shows the amount of methane combusted at each feed rate and the corresponding amount of oxygen consumed. We observe that as the flow rate of methane increases, the amount

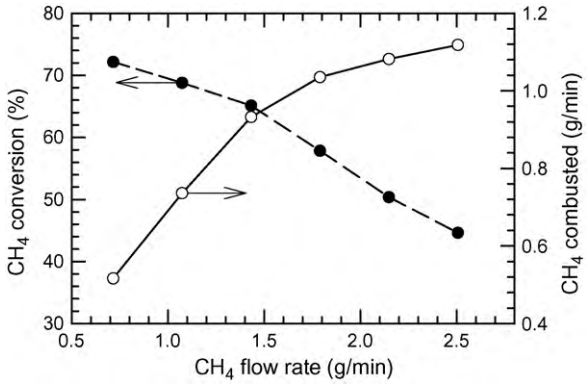

Fig. 5. Methane conversion and amount combusted at different feed rates.

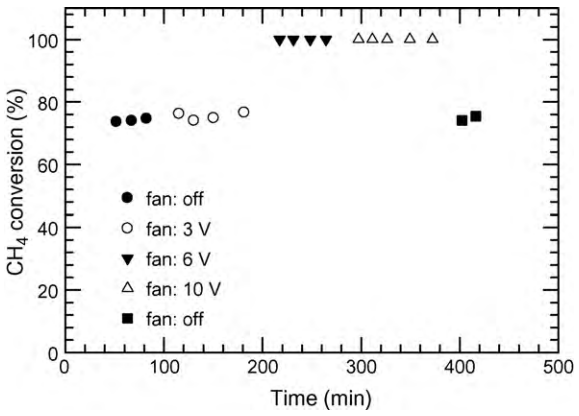

Fig. 6. Effect of fan speed on methane conversion at natural gas feed rate of 0.7 g/min.

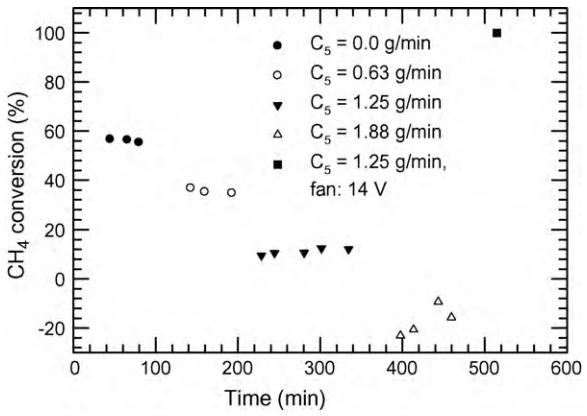

Fig. 7. Effect of addition of pentane on conversion of 1.8 g/min natural gas.

of methane combusted gradually rises (in spite of the decreasing conversion) until it reaches a plateau.

It is commonly accepted that, provided that the catalyst has sufficient activity, the limiting factor in conversion is oxygen diffusion. It is commonly assumed that the diffusion of oxygen in the pad is the mass transfer limiting step; however, it is equally plausible that the mass transfer through the boundary layer is the rate limiting step. To examine the role of external mass transfer of oxygen on the observed behavior, the fan on top of the hood was turned on. This should act to increase the flow of oxygen in front of the catalyst pad. The effect of oxygen supply on methane conversion is shown in Fig. 6. The methane conversion did not change at low fan speed; however, at high speeds, complete conversion of methane was achieved. Natural gas feed rate in this experiment was 0.7 g/min. When this experiment was performed at 1.8 g/min of feed gas, a higher fan speed (greater than 6 V applied), was required for complete oxidation. The main conclusion of this experiment is that oxygen transport in the boundary layer is the controlling step in combustion.

As mentioned previously, the catalyst pad is supported by a fibre cloth and it was suspected that the presence of cloth might have a negative impact on oxygen diffusion into the catalyst pad. Preliminary experiments showed that removing the fibre cloth did not have an effect on methane conversion. Therefore, all the experiments were conducted with the fibre cloth covering the catalyst pad. This observation would tend to support the observation that the rate limiting step is the transport of oxygen to the pad surface, rather than diffusion within the pad.

3.2. Effect of pentane addition

In this section, the results obtained from the injection of liquid non-methane hydrocarbons are reported (pentane and toluene). Eq. (2) was developed to calculate methane conversion in presence of pentane and toluene in the feed:

$$\text{CH}_4\ \text{conversion} = \frac{1 - (7X_7 + 5X_5)([\text{CH}_4]/[\text{CO}_2])}{1 + ([\text{CH}_4]/[\text{CO}_2])} \quad (2)$$

where $[CH_4]$ and $[CO_2]$ are the concentrations of methane and carbon dioxide in the exhaust from the reactor and X_7 and X_5 are the ratios of molar feed rates of toluene and pentane to methane, respectively. This equation reduces to Eq. (1) in the absence of pentane and toluene in the feed, and is predicated on the assumption that complete conversion of pentane and toluene occurs.

The first set of results was obtained by adding increasing amounts of liquid pentane. The methane flow rate was 1.8 g/min. Fig. 7 shows the methane conversion as a function of pentane injection rate. It was observed that as the flow rate of pentane increases, the conversion of methane decreases. This observation is consistent with the earlier one of decreasing methane conversion with increasing flow rate. In this experiment, we are effectively increasing the total oxygen demand (because the flow rate of methane was held constant), thus a decrease in methane conversion is expected. What is more significant is that there was essentially zero pentane detected in the reactor effluent until the pentane injection rate reached 1.88 g/min. At this point, the calculated methane conversion is negative, indicating that the pentane is not being completely combusted (as assumed in Eq. (2)), which is confirmed by the presence of pentane in the effluent. The major result of this experiment is that pentane is preferentially combusted, compared to methane. When at pentane flow rate of 1.25 g/min, fan was turned on it can be seen from Fig. 8 that complete conversion of methane is achieved.

In Fig. 4, the effect of increasing natural gas flow rate from 0.7 to 2.5 g/min on temperature distribution across the catalyst pad was shown. At lower methane flow rate, the heater would not remain ignited. For example, the temperature profile for a methane flow rate of 0.36 g/min is shown in Fig. 8. For the first 50 min, the electrical heater is on, and then, at about 50 min, natural gas is introduced into the reactor and the heater switched off. It is observed that all of the temperatures decline. It was attempted to reignite the radiant heater however the same pattern was observed. However, the addition of pentane and toluene as supplemental fuel allowed normal operation to be maintained. The reactor temperature profiles are shown in Fig. 9 for 0.36 g/min of natural gas with 0.57 g/min of pentane and toluene. Note that

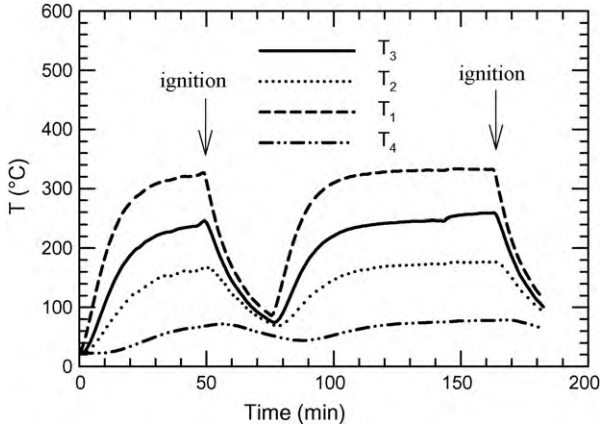

Fig. 8. Extinction of radiant heater at natural gas flow rate of 0.36 g/min.

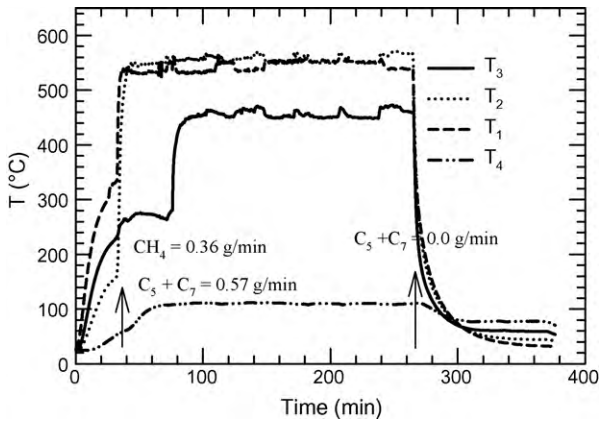

Fig. 9. Temperature profile across the catalyst pad at low natural gas flow rate with addition of pentane and toluene to the feed stream.

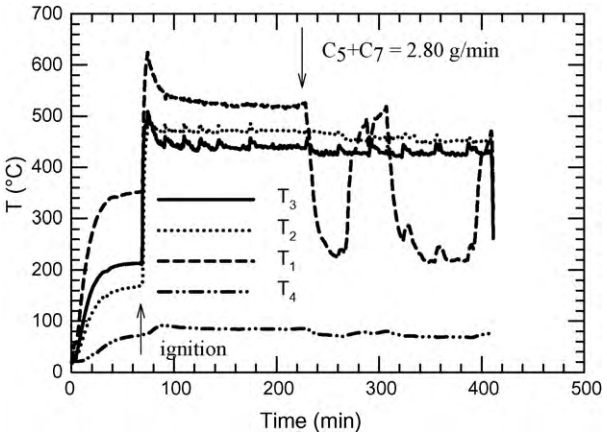

Fig. 10. Temperature profile across the catalyst pad at natural gas feed rate of 1.8 g/min in presence of C_5 and C_7 in the system.

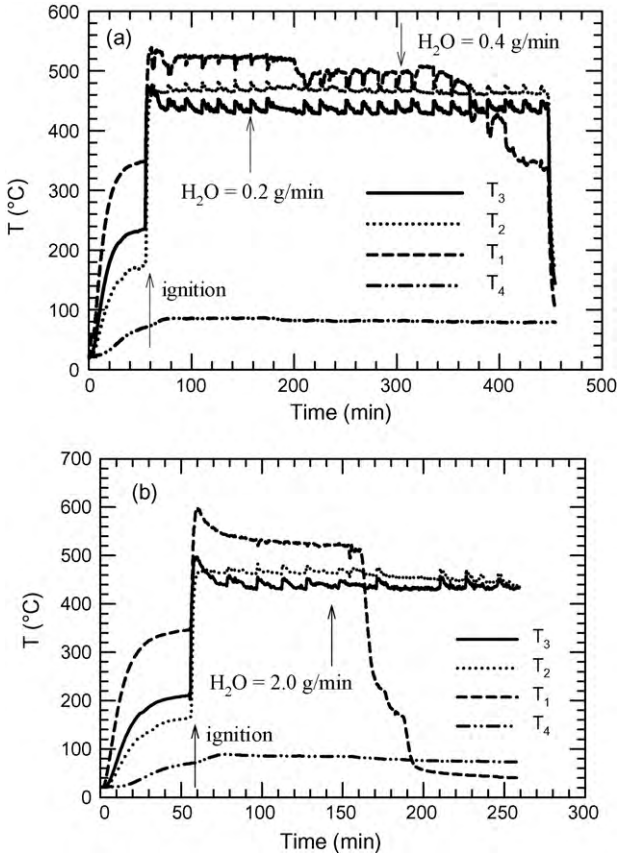

Fig. 11. Temperature profile across the catalyst pad at natural gas feed rate of 1.8 g/min in presence of (a) 0.2 and 0.4 g/min and (b) 2.0 g/min liquid water.

when the supplemental fuel supply is switched off at about 260 min, the reactor extinguishes.

When both pentane and toluene were added to the reactor, the same general trends were observed as with pentane alone. That is, increasing the supply of NMHC resulted in a reduction of methane conversion, and the NMHC are preferentially combusted. A further result of interest is obtained as the liquid injection rate was increased further than was reported in the preceding. At a total liquid injection of 2.8 g/min pentane and toluene with 1.8 g/min methane, the bottom of the catalyst pad was observed to start to cool down, as shown in Fig. 10. The lower corner temperature, T_1, drops quickly after C_5 and C_7 was added to the reactor feed. The sudden increase of temperature at 280 min was due to stopping the hydrocarbons flow to refill the syringe pump. After the flow starts again temperature at the bottom of the unit declined again. The same procedure was repeated at about 400 min; after 420 min, the reactor feed was stopped.

3.3. Effect of liquid water on radiant heater performance

A typical composition of the dehydrator effluent is given in Table 1. Approximately 40 vol.% of the feed is water, which is somewhat less than half as much again as is produced by the complete conversion of the other hydrocarbons in the mixture. To investigate the efficiency of radiant heater to combust such a mixture, the effect of addition of only liquid water was studied first, by continuously flowing different flow rates of water into the radiant heater at a methane feed rate of 1.8 g/min. Prior to the addition of water, enough time was allowed for the radiant heater to reach steady state. Temperature profiles across the catalyst pad at different water flow rates and corresponding methane conversion data are shown in Figs. 12 and 13, respectively. It is observed that the temperature profiles and methane conversion before addition of water are consistent in each run.

At water flow rate of 0.2 g/min, there was no significant change in the temperature profiles; however, the lower corner temperature, T_1, decreased when the water flow rate was increased to 0.4 g/min (see Fig. 11a). Further increases in the water flow rate to 1.0 and 2.0 g/min, resulted in large decreases in T_1 (see Fig. 11b). The catalyst pad became damp in the lower corner due to the condensation of water. When the water flow was stopped, the temperature profile fully recovered to its original state before water addition. The conversions at the different flow rates of water are summarized in Fig. 12. It is seen that at the lower flow rate the effect on conversion is small, and only becomes significant above 2.0 g/min. It should be noted that, although the addition rate of water may appear high, more water was produced during the oxidation of methane than was introduced even at the highest water flow rate. For example, 2.4 g/min of water is produced by methane oxidation at a natural gas feed rate of 1.8 g/min with a conversion of 60%.

In the literature, many results have been reported on the effect of water on methane conversion. Results have been discussed for both Pt and Pd catalysts. Burch et al. [12] studied the influence of addition of water and CO_2 to the feed stream of methane combustion system in a micro-reactor with palladium catalysts. He found that the effect of CO_2 was negligible and the decrease of catalyst activity is only due to water. By increasing the reaction

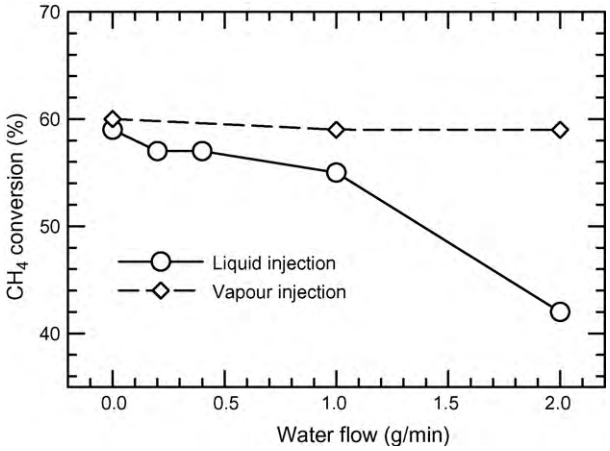

Fig. 12. Conversion of 1.8 g/min natural gas with an increasing injected rate of water.

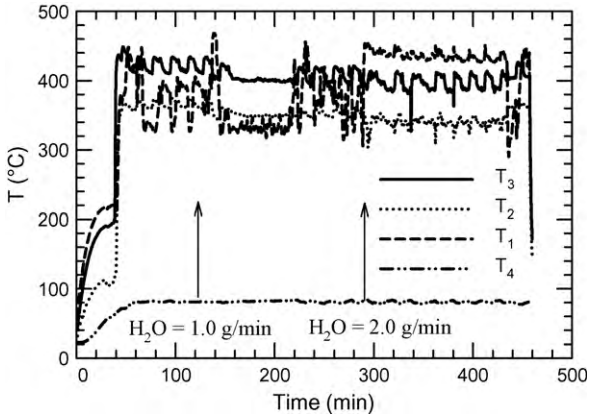

Fig. 13. Temperature profile across the catalyst pad at natural gas feed rate of 1.8 g/min with addition of water vapour to the system.

temperature and conversion, the effect of added water becomes negligible due to formation of more water during the reaction and lower stability of surface hydroxide at high temperatures. Gelin et al. [13] also studied the effect of addition of water vapour to the feed stream of methane oxidation system and found that Pd catalysts are sensitive to water and addition of 10 vol.% water strongly affects the activity of Pd catalyst due to competition of water and methane for active sites. In Urfels et al. [14] the activity of a Pt catalyst was observed to decline less than for Pd with water addition.

Cullis and Willat [15] reported that addition of water comparable to the amount produced during the reaction does not affect the Pd-based catalysts; van Giezen et al. [16] found that even high water concentrations will not influence the supported palladium catalyst activity. However, Reinke et al. [17] observed a significant inhibition by water of methane oxidation over Pt. That work studied high levels of water addition under turbine like conditions. Persson et al. [18] studied the effect of periodic water vapour addition on activity of Pd/Al_2O_3 and bimetallic $Pd–Pt/Al_2O_3$ and found that the bimetallic catalyst was not affected in the same extent as Pd/Al_2O_3 and Pt containing catalyst was less sensitive to water. Gelin et al. [13] also reported more significant loss of Pd activity compared to Pt. In another study conducted by Narui et al. [19] the effect of addition of Pt to $PdO/\alpha\text{-}Al_2O_3$ on catalytic activity was investigated and it was found that adding Pt not only resulted in increased catalytic activity, but it also prevented the catalyst deactivation during methane combustion. Growth of PdO particles (sintering) for $PdO/\alpha\text{-}Al_2O_3$ mentioned to be the reason for lower activity of $PdO/\alpha\text{-}Al_2O_3$. No change in activity was observed for catalysts with added Pt. Another investigation reports the promoting effect of water vapour on methane catalytic oxidation over Co/Mn mixed oxides [20].

3.4. Effect of water vapour on radiant heater performance

The effect on conversion at high water flow rate can be ascribed to either thermal effects (latent heat of vapourization) or to kinetic effects. It was seen that the injection of liquid water at high flow rate caused the temperature of the pad to decrease. In the real situation, water present in glycol regeneration effluent is in the vapour phase, thus a further set of experiments was undertaken to obtain more information about the radiant heater performance when water vapour rather than liquid water was fed to the system. Fig. 13 shows the temperature profile across the catalyst pad when 1.0 and 2.0 g/min water vapour were fed with 1.8 g/min of natural gas. It is seen that when water is added as a vapour, the temperature of the catalyst does not decrease, as was the case with liquid water feed (see Fig. 11). The methane conversion is shown in Fig. 12, where it is seen that the fractional conversion remains steady even at 2.0 g/min of water injected.

Because considerable energy is lost through the back and sides of the reactor (as evidenced by the relatively low back space temperature) the back wall and the sides of the radiant heater were insulated with fibre glass insulation blankets. The temperature profiles for the insulated reactor are shown in Fig. 14. Insulating the radiant heater increased the temperature in the back space of the reactor to about 200 °C. The methane conversion in this experiment was observed to be about 60% both in the presence and absence of water.

With the observation that the water vapour does not cause a loss in methane conversion, it is thus safe to conclude that the conversion loss observed in the water experiments is a result of thermal effects, and not kinetic effects. We cannot state that water addition does not cause a reduction in the kinetic reaction rate; however, this effect is apparently not significant for the conditions used here.

3.5. Effect of liquid water and hydrocarbons addition on radiant heater performance

The final results presented were obtained using mixtures most representative of the real glycol dehydrator effluent. The water,

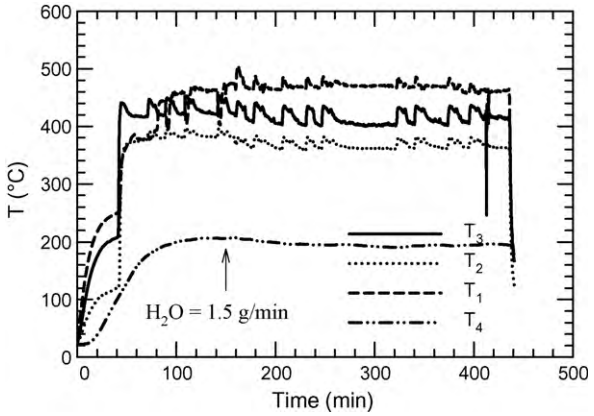

Fig. 14. Temperature profile across the catalyst pad at natural gas feed rate of 1.8 g/min in presence of water vapour after incomplete insulation of back and edges of the unit.

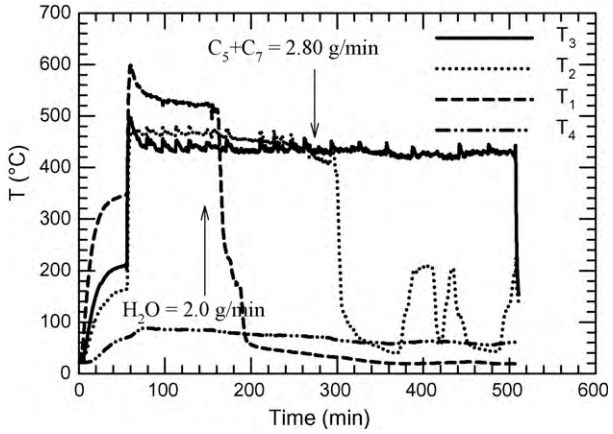

Fig. 15. Temperature profile across the catalyst pad at natural gas feed rate of 1.8 g/min in presence of liquid water, C_5 and C_7 in the system.

methane, pentane and toluene mixture used in the experiments consisted of 40 mol% methane, 40 mol% water, 17 mol% pentane and 3 mol% toluene.

Temperature profiles across the catalyst pad with addition of liquid water and hydrocarbons mixture are shown in Fig. 15. The temperature of the lower corner, T_1, dropped rapidly when the water feed was started and lower corner of the pad became damp. The temperature in the middle of the pad, T_2, declined rapidly after the heavy hydrocarbon flow was started. In fact, the addition of higher quantities of liquid compounds to the reactor resulted in the temperature in the back of the reactor (T_4) falling below the boiling point of toluene (see Fig. 15). The rise in temperature at 380, 420 and 480 min occurred when the heavy hydrocarbon feed was stopped temporarily. These results are expected, given the previous results from high loading levels of liquid water and NMHC.

Prior to the beginning of the injection of water, the methane conversion was 60%, as observed previously. With the addition of liquid water at 2.0 g/min, the methane conversion drop to about 42%, also the same value observed earlier. However, when the pentane and toluene flow was started, the methane conversion decreased to zero; the methane conversion calculated by Eq. (2) when pentane and toluene were in the feed was actually slightly less than zero indicating that not all the pentane and/or toluene was converted. Gas chromatographic analyses confirmed that there were traces of pentane and toluene in the exhaust gas. The incomplete combustion of the hydrocarbons was again due to oxygen diffusion limitation because complete conversions of methane, pentane and toluene were obtained when the fan was turned on.

4. Conclusions

This study has focused on the use of the counter-diffusive radiant heater as a tool for the destruction of BTEX emissions from a natural gas dehydrator. Based on the observations made, it can be concluded that the technology offers promise for this application. The primary limiting factor in the complete conversion of the hydrocarbon reactants is the transport of oxygen through the boundary layer at the catalyst pad face. Non-methane hydrocarbons are found to be preferentially combusted, compared to methane. Addition of water to the radiant heater did not affect the methane conversion; however, at higher water feed rates liquid water wetted the bottom of the catalyst pad. Introduction of water in the vapour phase eliminated this problem. In all cases, increasing the rate of oxygen transfer to the pad surface, via an induced forced convection boundary layer, enhanced the combustion, and in most cases was able to achieve complete conversion. On the basis of our results we conclude that the use of counter-diffusive radiant heaters, with some forced convection capabilities, is a feasible and economic option for treatment of glycol dehydrator effluent; not only can hazardous compounds be oxidized effectively but the thermal energy generated during the combustion can be recovered and used for other applications.

Acknowledgments

Financial support for this work was provided by the Natural Sciences and Engineering Research Council of Canada (NSERC) and the Canadian Association of Petroleum Producers (CAPP). Technical advice was provided by New Paradigm Engineering, Scott-Can Industries Ltd. and Husky Energy Inc.

References

[1] Environmental technology verification report, engineered concepts, LLC quantum leap dehydrator, prepared by Greenhouse Gas Technology Centre, Southern Research Institute, 2003.
[2] S. Su, J. Agnew, Fuel 85 (2006) 1201.
[3] S. Salomons, R.E. Hayes, M. Poirier, H. Sapoundjiev, Catal. Today 83 (2003) 59.
[4] A.K. Jorgenson, Soc. Forces 84 (2006) 1779.
[5] L. Liwi-Minsker, I. Yuranov, B. Siebenhaar, A. Renken, Catal. Today 54 (1999) 39.
[6] L. Kiwi-Minsker, I. Yuranov, E. Slavinskaia, V. Zaikovskii, A. Renken, Catal. Today 59 (2000) 61–68.
[7] Y.S. Seo, S.K. Kang, H.D. Shin, Int. J. Energy Res. 23 (1999) 543.
[8] Y.S. Seo, S.J. Cho, K.S. Song, S.K. Kang, Int. J. Energy Res. 26 (2002) 921.
[9] K.S. Fisher, C. Rueter, M. Lyon, J. Gamez, Oil Gas J. 93 (1995) 40.
[10] H. Sadamori, Catal. Today 47 (1999) 325.
[11] R.E. Hayes, N. Jodeiri, T. Manna, J. Mmbaga, S.E. Wanke, Recents Progres en Genie des Procedes 94 (2007) 1.
[12] R. Burch, F.J. Urbano, P.K. Loader, Appl. Catal. A: Gen. 123 (1995) 173.
[13] P. Gelin, L. Urfels, M. Primet, E. Tena, Catal. Today 83 (2003) 45.
[14] L. Urfels, P. Gelin, M. Primet, E. Tena, Top. Catal. 30/31 (2004) 427.
[15] C.F. Cullis, B.M. Willat, J. Catal. 86 (1984) 187.
[16] J.C. van Giezen, F.R. van den Berg, J.L. Kleinen, A.J. van Dillen, J.W. Geus, Catal. Today 47 (1999) 287.
[17] M. Reinke, J. Mantzaras, R. Bombach, S. Schenker, N. Tylli, Combust. Sci. Technol. 179 (2007) 553.
[18] K. Persson, L.D. Pfefferle, W. Schwartz, A. Ersson, S.G. Jaras, Appl. Catal. B: Environ. 74 (2007) 242.
[19] K. Narui, H. Yata, K. Furuta, A. Nishida, Y. Kohtoku, T. Matsuzaki, Appl. Catal. A: Gen. 179 (1999) 165.
[20] W. Li, Y. Lin, Y. Zhang, Catal. Today 83 (2003) 239.